

Importance of orbital fluctuations on magnetic dynamics in heavy fermion SmB₆

Christopher N. Singh* and Wei-Cheng Lee†

Binghamton University Department of Physics Applied Physics and Astronomy

(Dated: June 2, 2022)

The emergent dynamical processes associated with the magnetic excitations in heavy fermion SmB₆ are investigated. By imposing multi-orbital interactions on a first principles tight binding model, we find the interplay between magnetic and orbital fluctuations in the localized f -levels is highly sensitive to the Hubbard interaction U and the Hund's coupling J . The magnetic phase diagram constructed at zero temperature reveals novel quantum critical features with the existence of several competing magnetic phases. Within the random phase approximation, we perform a comprehensive study of the spin-spin correlation function, and our results agree with the neutron scattering experiments. Furthermore, analysis of the spectral weight of the magnetic excitations shows that some collective spin excitations are accompanied by orbital fluctuations, indicating an interesting entanglement between the spin and the orbital degrees of freedom in SmB₆. Our work underscores the importance of the orbital degrees of freedom in the physics of heavy fermion systems.

Introduction – A unified theoretical framework to treat correlated electronic systems has been the coveted focus of many researchers in condensed matter physics. The interplay of competing energy scales and many degrees of freedom invoke rich phase diagrams and striking electronic properties. It is well known the Coloumb interaction, lattice geometry, and spin orientation are essential, however fair treatment of multi-orbital systems is often hindered by an exponential growth in complexity.

While the possibility that SmB₆ is topologically non-trivial has driven a lot of recent research efforts [1–12], another important aspect of this material has been brought under scrutiny through the lens of inelastic magnetic neutron scattering (INS). Several mysterious temperature activated magnetic excitations which are highly anisotropic in momentum space have been observed near 14meV [13–15]. Identifying the origin of these low energy modes as well as the interplay between correlation and topology is crucial in understanding SmB₆, but a comprehensive theoretical study on the magnetic dynamics is still lacking.

In ths Letter, we address this gap with a realistic model based on complementing Density Functional Theory (DFT) with the generalized random phase approximation (GRPA). This is acheived by projecting the relativistic eigenstates of the Kohn-Sham equations onto Wannier functions, and imposing the multi-orbital Hubbard (Kanamori) interactions onto the maximally localized orbitals. This model allows us to treat the spin-orbit coupling, multi-orbital Coulomb interactions, and Fermi surface effects on equal footing. We show that SmB₆ is highly quantum critical at zero temperature with several nearby magnetic phases. In the normal state at finite temperatures, the low-energy spin excitations are found to be tightly coupled to orbital exchange processes through the large spin-orbit coupling, and a number of important features observed in the INS experiments can be reproduced within our theory, highlighting the importance of orbital fluctuations in the physics of heavy

fermion systems.

Model – Motivated to capture hybridization effects between localized Sm $4f$ moments, and itinerant Sm $5d$ states, we define a generalized multi-orbtial Hamiltonian

$$H = H_t + H_{int} \quad (1)$$

where H_t is given by

$$H_t = \frac{1}{2} \sum_{ij\alpha\beta\sigma} (t_{ij}^{\alpha\beta} - 2\mu\delta_{ij}\delta_{\alpha\beta}) c_{i\alpha\sigma}^\dagger c_{j\beta\sigma} \quad (2)$$

Here the fermion operators create (destroy) particles at site i (j), with orbital character α (β) and spin σ . H_t represents the single particle spectrum and is completely determined from the first principles calculation. With the inclusion of symmetry considerations [16] and the spin-orbit interaction, a Wannier basis is chosen as spinors of the Sm d - eg states and the full Sm f level multiplet. Contained within H_t is the fully relativistic ab inito information pertaining to the entirety of the Kondo hybridization, as well as f level character in the vicinity of the Fermi surface.

$$\begin{aligned} H_{int} = & \frac{U}{2} \sum_{i\alpha\sigma} n_{i\alpha\sigma} n_{i\alpha\sigma} \\ & + \sum_{i,\alpha<\beta,\sigma} \{ (U - 2J) n_{i\alpha\sigma} n_{i\beta\sigma} + (U - 3J) n_{i\alpha\sigma} n_{i\beta\sigma} \\ & + J (c_{i\alpha\sigma}^\dagger c_{i\beta\sigma} c_{i\beta\sigma}^\dagger c_{i\alpha\sigma} - c_{i\alpha\sigma}^\dagger c_{i\beta\sigma} c_{i\alpha\sigma}^\dagger c_{i\beta\sigma}) \} \end{aligned} \quad (3)$$

H_{int} is the centrosymmetric representation [17] of the multi-orbital Hubbard (Kanamori) interaction [18] that will be employed at the mean field level to calculate the magnetic phase diagram, and at the RPA level to calculate the dynamical spin-susceptibility in the normal state. U is the intra-orbital repulsion, and J is the Hund's coupling parameter. The first principles calculations are performed with full potential linear augmented plane waves plus local orbitals (FP-LAPW+lo) and the local density

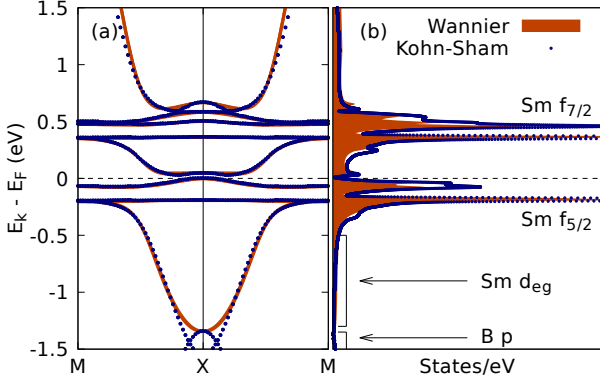


FIG. 1. Electronic structure plots contrasting LDA and Wannier projection. (a) bandstructure (b) density of states

approximation (LDA) provided in WIEN2k [19]. The total energy was converged to 0.1 meV on a 5000 kpoint grid with an RKmax of 5. Projection onto Wannier states including fourth nearest neighbors is accomplished with the Wannier90 package [20].

Figure (1) overlays the Wannier interpolated electronic structure with the Kohn-Sham result. The density of states shows the sharp Sm f peaks with the doubly split $J = 5/2$ and triply split $J = 7/2$ multiplets just below and above the Fermi level respectively [16]. This electronic structure is representative of a weak cubic field and strong spin-orbit coupling scheme [21]. The multiplet electronic structure in our model agrees with the most recent tunneling data [22]. The itinerant Sm d - eg bands are seen to hybridize with the localized f manifold across a 15 meV gap. Excellent agreement is found between the Wannier projection and Kohn-Sham result in the low energy window $E_f \pm 500$ meV. Admittedly, a parity crossing between the hybridized Samarium $4f$ band and the Boron p at the X point lost in this Wannier projection, resulting in a shift of the Berry phase. However, being interested in Fermi surface effects, our truncated basis serves as an effective representation of the low energy physics.

Mean Field Theory – Decoupling the quartic terms in the interaction is accomplished with the standard assumption [23, 24]

$$\langle c_{i\alpha\sigma}^\dagger c_{j\beta\sigma'} \rangle = [n_\alpha + \frac{\sigma}{2} \cos(\mathbf{q} \cdot \mathbf{r}_i) m_\alpha] \delta_{ij} \delta_{\alpha\beta} \delta_{\sigma\sigma'} \quad (4)$$

This leads to a momentum space mean field Hamiltonian

$$H^{MF} = H_t + \sum_{\mathbf{p}\alpha\sigma} \theta_\alpha c_{\mathbf{p}\alpha\sigma}^\dagger c_{\mathbf{p}\alpha\sigma} + \zeta + \sum_{\mathbf{p}\alpha\sigma} \eta_{\alpha\sigma} (c_{\mathbf{p}\alpha\sigma}^\dagger c_{\mathbf{p}+\mathbf{q}\alpha\sigma} + h.c) \quad (5)$$

with mean field potentials

$$\begin{aligned} \theta_\alpha &= U n_\alpha + (2U - 5J) \sum_{\beta \neq \alpha} n_\beta \\ \eta_{\alpha\sigma} &= -\frac{\sigma}{2} (U m_\alpha + J \sum_{\beta \neq \alpha} m_\beta) \end{aligned} \quad (6)$$

and mean field constant

$$\begin{aligned} \zeta &= \frac{J}{2} \sum_{\alpha \neq \beta} m_\alpha m_\beta - U \sum_{\alpha} (n_\alpha^2 - \frac{1}{4} m_\alpha^2) \\ &\quad - (2U - 5J) \sum_{\alpha \neq \beta} n_\alpha n_\beta \end{aligned} \quad (7)$$

Calculating the phase diagram proceeds by self-consistently determining the mean field parameters n_α and $m_\alpha = n_{\alpha\uparrow} - n_{\alpha\downarrow}$, with convergence characterized by $\|D\| < 1 \times 10^{-5}$.

$$D = \langle n_{i+1}^\alpha - n_i^\alpha \rangle \langle m_{i+1}^\alpha - m_i^\alpha \rangle \quad (8)$$

Minimization of the norm of D gives the self-consistent condition, automatically ensuring a minimum in the free energy [25]. The self-consistent process is repeated across different magnetic phases and ordering wavevectors. We consider a set of 5 phases characterized by 3 antiferromagnetic ordering wavevectors $\mathbf{q}_1 = (\frac{1}{2}, 0, 0)$, $\mathbf{q}_2 = (\frac{1}{2}, \frac{1}{2}, 0)$, $\mathbf{q}_3 = (\frac{1}{2}, \frac{1}{2}, \frac{1}{2})$, and the paramagnetic and ferromagnetic phases. The total particle number is constrained to the experimental average Sm valence of 2.54 [26] during each of the self-consistency cycles.

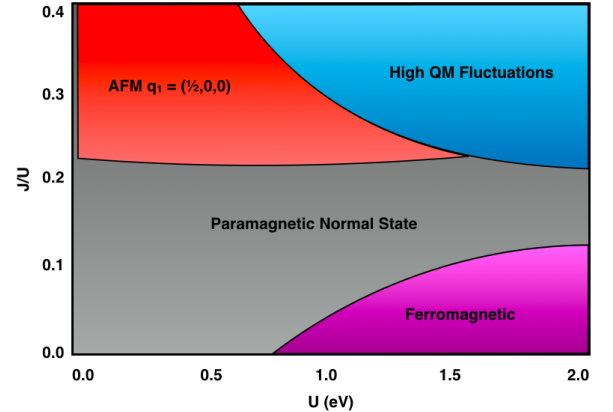


FIG. 2. Schematic magnetic phase diagram of SmB₆ obtained by mean-field treatment of first principles Wannier projection.

Figure (2) shows the zero temperature magnetic phase diagram in the plane of the interaction parameters U and J . A central feature consistent with μ SR experiments [27] is the large paramagnetic belt found in the region with moderate correlations where the intra-orbital repulsion is comparable to the f level bandwidth W . Interestingly, in the regime of large Hund's coupling J compared

to intra-orbital repulsion U , $\mathbf{q}_1 = (\frac{1}{2}, 0, 0)$ antiferromagnetic order is found to be the groundstate. We notice that high pressure experiments [28] have already seen some evidence for this 1-D like antiferromagnetic order, and a recent theoretical study reported in Ref. [29] has obtained similar results as well. The region of $U > 1\text{eV}$, $J/U > 1/5$ shows several phases very close in energy, suggesting the dominance of quantum fluctuations and highly competing order. For $U \gg J/U$, ferromagnetism is found to be the lowest-energy magnetic phase. It is worth mentioning that experimental evidence for ferromagnetic order is not conclusive. While μSR experiments [27] find no evidence of long range ferromagnetic order, magnetoresistance experiments [30] are suggestive of ferromagnetic puddling. In short, our mean-field calculations have shown that various competing magnetic orders exist in SmB_6 at zero temperature, implying that the magnetic dynamics might be complicated even in the normal state at finite temperatures.

Spin Susceptibility – In order to deepen our understanding of the spin dynamics in multi-orbital spin-orbit coupled systems, we study the magnetic excitations in the normal state with the following correlation tensor

$$\hat{\chi}_{\alpha\alpha'\beta\beta'}^{\gamma\delta}(\mathbf{q}, i\omega_n) = \int_0^\beta d\tau e^{i\omega_n\tau} \langle T_\tau m_{\alpha\alpha'}^\gamma(\mathbf{q}, \tau) m_{\beta\beta'}^\delta(-\mathbf{q}, 0) \rangle \quad (9)$$

where

$$m_{\alpha\alpha'}^z(\mathbf{q}, \tau) = \sum_{\mathbf{p}\sigma} \sigma c_{\mathbf{p}+\mathbf{q}\alpha}^\dagger(\tau) c_{\mathbf{p}\alpha'}(\tau) \quad (10)$$

The lower greek indices represent orbitals and the upper indices represent magnetization direction components. Evaluation of the correlation tensor follows textbook procedures [31], and the bare susceptibility can be expressed by the generalized Lindhard function

$$\begin{aligned} \chi_{\bar{\alpha}\bar{\beta}}^{zz}(\mathbf{q}, \omega) &= \frac{1}{2N} \sum_{\mathbf{p}\sigma} \sigma \Xi_{\bar{\alpha}\bar{\beta}}^{ab\sigma}(\mathbf{p}, \mathbf{q}) \Lambda_{ab}(\mathbf{p}, \mathbf{q}, \omega) \\ \Xi_{\bar{\alpha}\bar{\beta}}^{ab\sigma}(\mathbf{p}, \mathbf{q}) &\equiv (U_{\alpha a \sigma}^{\mathbf{p}+\mathbf{q}})^* U_{\alpha' b \sigma}^{\mathbf{p}} (U_{\beta b \sigma}^{\mathbf{p}})^* U_{\beta' a \sigma}^{\mathbf{p}+\mathbf{q}} \\ \Lambda_{ab}(\mathbf{p}, \mathbf{q}, \omega) &\equiv \frac{n_F(\xi_{\mathbf{p}+\mathbf{q}a}) - n_F(\xi_{\mathbf{p}b})}{\omega + i\eta + \xi_{\mathbf{p}b} - \xi_{\mathbf{p}+\mathbf{q}a}} \end{aligned} \quad (11)$$

where contravariant indices are band indices and are summed over, Ξ is the orbital projection weight, and Λ gives the thermal occupations [32]. Here the rank four tensor is operated as a matrix by defining the sets $\bar{\alpha} = \{\alpha, \alpha'\}$ and $\bar{\beta} = \{\beta, \beta'\}$. Due to the presence of strong spin-orbit coupling, the longitudinal (χ^{zz}) and transverse (χ^\pm) functions are calculated separately since they could be different. Within the GRPA, the renormalized correlation functions become

$$\begin{aligned} \chi_{\bar{\alpha}\bar{\beta}}^{zz} &= \chi^1 + \chi^4 - \chi^2 - \chi^3 \\ \chi_{\bar{\alpha}\bar{\beta}}^\pm &= \chi^5 \end{aligned} \quad (12)$$

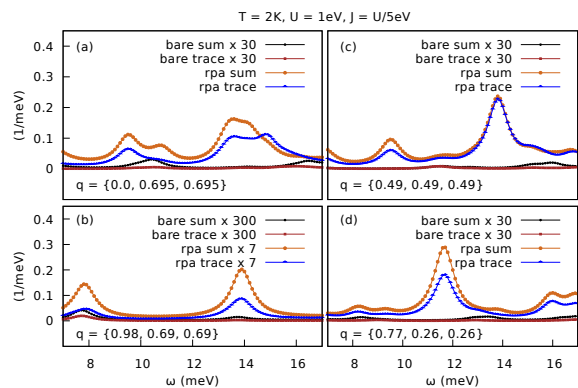


FIG. 3. Longitudinal spin response spectrum for selected scattering vectors of INS data. Note the spectra have been scaled differently. In this plot $T = 2\text{K}$, $U = 1\text{eV}$, $J = U/5$

The functions χ^{1-5} , along with the interaction kernel are worked out in detail in Refs. [33, 34]. The spectral function of this correlator is directly measured by INS experiments. What is known from experiment is the low energy peaks around 14 meV cannot be attributed to phonon, crystal field, or pure magnon modes [13]. To gain insight into the origin of these peaks, we analyze the orbital components of these peaks around 14 meV for a set of scattering vectors tested by Ref. [13]. The GRPA calculations were performed on a 1000 k -point grid in the full Brillouin zone with a thermal broadening factor $\eta = 0.5$ meV.

TABLE I.

Function	Orbital conservation
$\sum_{\bar{\alpha}\bar{\beta}} (\chi_{\bar{\alpha}\bar{\beta}}^\pm)$	No
$\sum_{\bar{\alpha}\bar{\beta}} (\chi_{\bar{\alpha}\bar{\beta}}^{zz})$	No
$\text{tr}(\chi_{\bar{\alpha}\bar{\beta}}^\pm)$	Yes
$\text{tr}(\chi_{\bar{\alpha}\bar{\beta}}^{zz})$	Yes

Fig. 3 shows two examples of orbital decompositions of the spectral function extracted via the sum and the trace of the longitudinal function from Eqn. 12. We start from the comparison between the bare and GRPA susceptibilities. In Fig. 3a, the bare function shows no signature at 14 meV whereas the GRPA produces the peaks matching the INS data, which means these modes are a result of electron correlations instead of Fermi surface nestings. Furthermore, the difference between the sum and the trace of the correlation function can be used to determine orbital components in the peaks. If the sum and the trace have nearly identical line-shapes, the corresponding peak is mainly associated with spin-flip processes within intra-orbital channels. In this case, the orbital fluctuations do not couple to this spin mode. On the other hand, if the trace is only a small part in the

sum around an INS peak, the corresponding peak is predominantly in the inter-orbital channels, and the orbital fluctuations would be strongly entangled with this spin mode. Table I summarizes how the correlation tensor is used to classify processes depending on initial and final orbital states. Comparing the spin-spin correlation functions at four different momenta plotted in Fig. 3, we find that the magnetic excitations at $q = (0, 0.695, 0.695)$, $(0.98, 0.69, 0.69)$ and $(0.77, 0.26, 0.26)$ have larger inter-orbital components while those at $q = (0.49, 0.49, 0.49)$ are mainly in the intra-orbital channels. This observation indicates that the effects of the interactions driving the spin collective modes near 14 meV are inhomogeneous throughout the momentum space, despite the fact that SmB_6 has a centrosymmetric crystal structure. This strongly suggests that orbital degrees of freedom play a crucial role not only on the Fermi surfaces but also on the collective excitations emerging from electron correlations.

Fig. 4a and 4b maps the transverse spin excitation in ω - q space. The inter vs intra orbital channels can be seen to have different structure in momentum space. This reiterates a strong inhomogeneity in the spin-orbital coupling, and leads us to conclude the Fermi surface is selectively susceptible to orbital deformations. The peak around $q = X$ observed in INS and in our data can be directly tied to the phase diagram, as this excitation is associated with 1D AFM order. The fact that we find the X point susceptibility peaking near 4meV is indicative that in our model, the cost of the 1D AFM excitation is within 10meV of experiment.

Fig. 5a and 5b plot the longitudinal susceptibility as a function of U with $J = U/5$ for the selected scattering vector $q = (0, 0.695, 0.695)$. We find that the excitation at 14 meV onsets as $U \approx W \approx 1\text{eV}$. While this result agrees with the previous study [15, 35], our results further ascribed significant orbital angular momentum to the spectral weight of the 14 meV mode. The fact that the 14 meV peak arises when $U \approx W$ places a strong constraint on theoretical treatment of correlations in SmB_6 .

Conclusion – We have shown that a first principles tight binding model can reproduce the low energy physics in SmB_6 , and that momentum dependent entanglement between the spin the the orbital degrees of freedom emerges naturally from strong spin-orbit coupling. We have shown that various competing magnetic phases exist at the zero temperature, leading to non-trivial magnetic dynamics even in the normal state. By studying the spectral decomposition of the spin susceptibility, we find that the spin-orbital character of the excitations is anisotropic in momentum space, and our model reproduces accurately a number of intriguing features observed in the inelastic neutron scattering measurement. With the evidence presented here, we propose that the orbitally degenerate non-dispersive f manifold is the perfect environment to harbor *orbital exciton* modes, meaning the

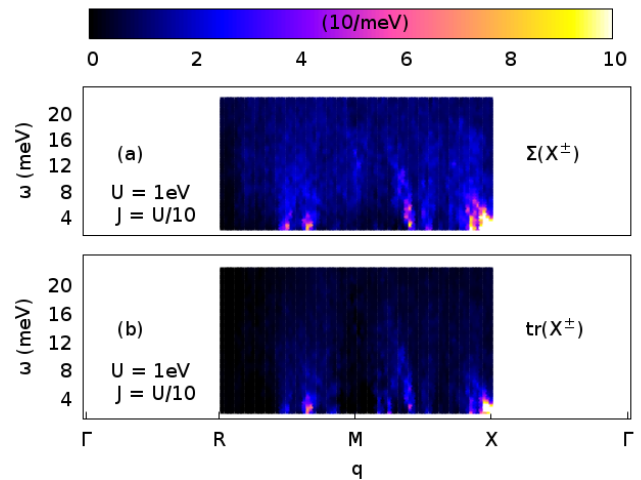


FIG. 4. (top) The sum of the transverse function for $T = 5\text{K}$, $U = 1\text{eV}$, $J = U/10$. (bottom) trace of the transverse function for $T = 5\text{K}$, $U = 1\text{eV}$, $J = U/10$.

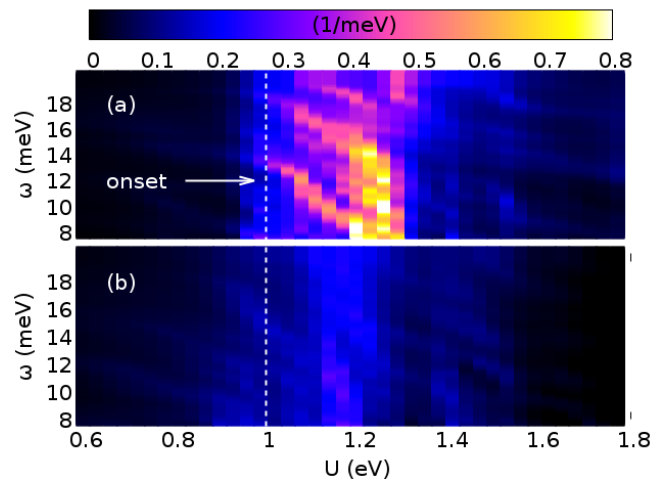


FIG. 5. Scattering at $q = (0, 0.695, 0.695)$ as a function of interaction. (top) The sum of the longitudinal function for $T = 2\text{K}$, $J = U/5$. (bottom) trace of the longitudinal function for $T = 2\text{K}$, $J = U/5$.

exciton would exclusively carry orbital angular momentum. This conjecture presents a new physical interpretation when considering non-trivial topology with a charge-neutral Fermi surface, and provides a simple mechanism for bulk SmB_6 to couple selectively to magnetic perturbations, while ignoring charge perturbations. Further work to address this issue is in progress.

Acknowledgements – This work utilized the Extreme Science and Engineering Discovery Environment (XSEDE) supported by National Science Foundation grant number ACI-1548562. It was also supported by a Binghamton University start up fund. The authors thank Pegor Aynajian for discussions regarding INS and Feliciano Giustino for discussions regarding DFT.

-
- * email at: csingh5@binghamton.edu; visit webpage at: <http://www.linkedin.com/in/csingh5binghamton/>
- † email at: wlee@binghamton.edu; visit webpage at: <http://bingweb.binghamton.edu/~wlee/>
- [1] A. Menth, E. Buehler, and T. H. Geballe, *Phys. Rev. Lett.* **22**, 295 (1969).
- [2] L. Kouwenhoven and L. Glazman, (2001), [arXiv:cond-mat/0104100](https://arxiv.org/abs/cond-mat/0104100).
- [3] M. C. Hatnean, M. R. Lees, D. M. Paul, and G. Balakrishnan, *Scientific Reports* **3**, 3071 (2013).
- [4] M. Dzero, K. Sun, V. Galitski, and P. Coleman, *Phys. Rev. Lett.* **104**, 106408 (2010).
- [5] S. Wolgast, C. Kurdak, K. Sun, J. W. Allen, D.-J. Kim, and Z. Fisk, *Phys. Rev. B* **88**, 180405 (2013).
- [6] D. Kim, S. Thomas, T. Grant, J. Botimer, Z. Fisk, and J. Xia, *Scientific Reports* **3** (2013).
- [7] D. J. Kim, J. Xia, and Z. Fisk, *Nature Materials* **13**, 466 (2014).
- [8] M. Neupane, N. Alidoust, S. Xu, T. Kondo, Y. Ishida, D.-J. Kim, C. Liu, I. Belopolski, Y. Jo, T.-R. Chang, *et al.*, *Nature Communications* **4**, 2991 (2013).
- [9] N. Xu, P. Biswas, R. Dhaka, G. Landolt, S. Muff, C. Matt, X. Shi, N. Plumb, M. Radovic, E. Pomjakushina, *et al.*, *Nature Communications* **5** (2014).
- [10] N. Wakeham, P. F. S. Rosa, Y. Q. Wang, M. Kang, Z. Fisk, F. Ronning, and J. D. Thompson, *Phys. Rev. B* **94**, 035127 (2016).
- [11] G. Li, Z. Xiang, F. Yu, T. Asaba, B. Lawson, P. Cai, C. Tinsman, A. Berkley, S. Wolgast, Y. S. Eo, D.-J. Kim, C. Kurdak, J. W. Allen, K. Sun, X. H. Chen, Y. Y. Wang, Z. Fisk, and L. Li, *Science* **346**, 1208 (2014).
- [12] B. Tan, Y.-T. Hsu, B. Zeng, M. C. Hatnean, N. Harrison, Z. Zhu, M. Hartstein, M. Kiourlappou, A. Srivastava, M. Johannes, *et al.*, *Science* **349**, 287 (2015).
- [13] P. Alekseev, J. Mignot, J. Rossat-Mignod, V. Lazukov, I. Sadikov, E. Kononova, and Y. B. Paderno, *Journal of Physics: Condensed Matter* **7**, 289 (1995).
- [14] P. Nyhus, S. L. Cooper, Z. Fisk, and J. Sarrao, *Phys. Rev. B* **55**, 12488 (1997).
- [15] W. T. Fuhrman, J. Leiner, P. Nikolić, G. E. Granroth, M. B. Stone, M. D. Lumsden, L. DeBeer-Schmitt, P. A. Alekseev, J.-M. Mignot, S. M. Koohpayeh, P. Cottingham, W. A. Phelan, L. Schoop, T. M. McQueen, and C. Broholm, *Phys. Rev. Lett.* **114**, 036401 (2015).
- [16] C.-J. Kang, J. Kim, K. Kim, J. Kang, J. D. Denlinger, and B. I. Min, *Journal of the Physical Society of Japan* **84**, 024722 (2015).
- [17] The centrosymmetric approximation is used for simplicity, but some recent evidence [36] suggests that a more detailed treatment of the inter-orbital interaction may be pertinent.
- [18] J. Kanamori, *Progress of Theoretical Physics* **30**, 275 (1963).
- [19] P. Blaha, K. Schwarz, G. Madsen, D. Kvasnicka, and J. Luitz, *An augmented plane wave+ local orbitals program for calculating crystal properties* (2001).
- [20] A. A. Mostofi, J. R. Yates, G. Pizzi, Y.-S. Lee, I. Souza, D. Vanderbilt, and N. Marzari, *Computer Physics Communications* **185**, 2309 (2014).
- [21] M. Tinkham, *Group Theory and Quantum Mechanics* (Courier Corporation, 2003) p. 79.
- [22] Z. Sun, A. Maldonado, W. S. Paz, D. S. Inosov, A. P. Schnyder, J. J. Palacios, N. Y. Shitsevalova, V. B. Filipov, and P. Wahl, (2018), [arXiv:1803.08776](https://arxiv.org/abs/1803.08776).
- [23] T. Nomura and K. Yamada, *Journal of the Physical Society of Japan* **69**, 1856 (2000).
- [24] E. Dagotto, A. Moreo, A. Nicholson, Q. Luo, S. Liang, and X. Zhang, *Frontiers of Physics* **6**, 379 (2011).
- [25] D. D. Johnson, *Phys. Rev. B* **38**, 12807 (1988).
- [26] Y. Utsumi, D. Kasinathan, K.-T. Ko, S. Agrestini, M. W. Haverkort, S. Wirth, Y.-H. Wu, K.-D. Tsuei, D.-J. Kim, Z. Fisk, A. Tanaka, P. Thalmeier, and L. H. Tjeng, *Phys. Rev. B* **96**, 155130 (2017).
- [27] P. K. Biswas, Z. Salman, T. Neupert, E. Morenzoni, E. Pomjakushina, F. von Rohr, K. Conder, G. Balakrishnan, M. C. Hatnean, M. R. Lees, D. M. Paul, A. Schilling, C. Baines, H. Luetkens, R. Khasanov, and A. Amato, *Phys. Rev. B* **89**, 161107 (2014).
- [28] A. Barla, J. Derr, J. P. Sanchez, B. Salce, G. Laperot, B. P. Doyle, R. Ruffer, R. Lengsdorf, M. M. Abd-Elmeguid, and J. Flouquet, *Phys. Rev. Lett.* **94**, 166401 (2005).
- [29] K.-W. Chang and P.-J. Chen, “The anomalous antiferromagnetic topological phase in pressurized Sb_2Te_3 ,” (2017), [arXiv:1710.10423](https://arxiv.org/abs/1710.10423).
- [30] Y. Nakajima, P. Syers, X. Wang, R. Wang, and J. Paglione, *Nature Physics* **12**, 213 (2016).
- [31] G. D. Mahan, *Many-Particle Physics* (Springer Science & Business Media, 2013).
- [32] See appendix for definitions.
- [33] X. Wu, F. Yang, C. Le, H. Fan, and J. Hu, *Physical Review B* **92**, 104511 (2015).
- [34] S. Mukherjee and W.-C. Lee, *Physical Review B* **94**, 064407 (2016).
- [35] W. T. Fuhrman and P. Nikolić, *Phys. Rev. B* **90**, 195144 (2014).
- [36] Z. Xiang, B. Lawson, T. Asaba, C. Tinsman, L. Chen, C. Shang, X. H. Chen, and L. Li, *Phys. Rev. X* **7**, 031054 (2017).